Chemical stability and H_2 flux degradation of cercer membranes based on lanthanum tungstate and lanthanum chromite

Jonathan M. Polfus[a*], Zuoan Li[a], Wen Xing[a], Martin F. Sunding[a], John C. Walmsley[a], Marie-Laure Fontaine[a], Partow P. Henriksen[a], Rune Bredesen[a]

[a]SINTEF Materials and Chemistry, Forskningsveien 1, NO-0314 Oslo, Norway

*Contact email: jonathan.polfus@sintef.no

Keywords: Hydrogen separation; Dense ceramic membrane; Ceramic–ceramic composite; Lanthanum tungstate; Lanthanum chromite;

Abstract

Ceramic-ceramic composite (cercer) membranes of (Mo-doped) lanthanum tungstate, $La_{27}(W,Mo)_5O_{55.5-\delta}$, and lanthanum chromite, $La_{0.87}Sr_{0.13}CrO_{3-\delta}$, have recently been shown to exhibit H_2 permeabilities among state-of-the-art. The present work deals with the long-term stability of these cercer membranes in line with concern of flux degradation and phase instability observed in previous studies. The H_2 permeability of disc shaped membranes with varying La/W ratio in the lanthanum tungstate phase ($5.35 \leq La/W \leq 5.50$) was measured at 900 and 1000 °C with a feed gas containing 49% H_2 and 2.5% H_2O for up to 1500 hours. It was observed that the H_2 permeability decreased by a factor of up to 5.3 over 1500 hours at 1000 °C. Post-characterization of the membranes and similarly annealed samples was performed by SEM, STEM and XRD, and segregation of La_2O_3 was observed. The decrease in H_2 permeability was ascribed to the compositional instability of the cation-disordered lanthanum tungstate under the measurement conditions. Equilibration of the La/W ratio by segregation of La_2O_3 leads to a lower ionic conductivity according to the materials inherent defect chemistry. Partial decomposition and reduction of the lanthanum tungstate phase, presumably to metallic tungsten, was also observed after exposure to nominally dry hydrogen.

1. Introduction

Hydrogen permeable membranes are applicable in power generation processes with pre-combustion CO_2 capture and for production of hydrogen and valuable chemicals in catalytic membrane reactors [1–6]. Dense ceramic membranes are of particular interest due to their potential stability under conditions relevant for processes at temperatures above 700 °C. Further development of such membranes involves improving H_2 flux and validation of their chemical and thermo-mechanical stability at operating conditions.

Hydrogen permeation through dense ceramic membranes proceeds according to ambipolar transport of protons and electronic charge carriers; the H_2 flux will be limited by the species with the lowest partial conductivity as described by the ambipolar transport [7]. Oxide ion transport can also yield H_2 in the permeate side of the membrane by splitting of H_2O in wet sweep gas due to oxide ion transport to the feed side driven by an oxygen chemical potential gradient [8,9].

Ceramic-ceramic composites (cercer) that exhibit mixed ionic-electronic conduction have recently attracted considerable attention due to the challenge for a single-phase material to show optimal electrical properties, and due to microstructural stability and thermo-mechanical compatibility issues with ceramic-metal composites. Notable examples of cercer membranes include composites of proton conducting $SrZrO_3$ and electronically conducting $SrFeO_3$ [10], and those of proton conducting Ca-doped $LaNbO_4$ and electronically conducting

$LaNb_3O_9$ [11]. In this work, we focus on the lanthanum tungstate – lanthanum chromite system which has recently been reported to exhibit chemical compatibility and high H_2 permeabilities [12,13].

Lanthanum tungstate with compositions close to $3(La_2O_3)\cdot(WO_3)$ exhibits rather high proton conductivity at intermediate temperatures of 500-700 °C and hydrogen containing atmospheres, and can also show appreciable electronic conductivity if appropriately doped with transition metals such as Mo or Re [14–16]. While lanthanum tungstate is stable as several compositions according to stoichiometric combinations of $(La_2O_3)\cdot(WO_3)$: $La_{10}W_2O_{21}$ (5:2), $La_6W_2O_{15}$ (3:2) and La_2WO_6 (1:1) – in addition to equivalent lanthanide compositions – single phase material has been reported for La/W ratios in the range 5.3-5.7 and not for a nominal 6.0 ratio corresponding to $3(La_2O_3)\cdot(WO_3)$ [17]. Considerable efforts have been directed towards understanding the crystallographic structure and non-stoichiometry of the latter composition, which involves both cation and anion disorder: the fluorite related structure contains excess W substituted on La sites and inherent oxide-ion disorder (see Figure 1) [17–20]. Tungsten substituted on lanthanum sites will have triply positive effective charge, $W_{La}^{\bullet\bullet\bullet}$ in Kröger-Vink notation, and reduce the number of oxygen vacancies, $v_O^{\bullet\bullet}$, according to electroneutrality. The formula unit may therefore be written $La_{28-x}W_{4+x}O_{54+3x/2-\delta}v_{2-3x/2}$, where x quantifies W substituted on La sites and v denotes inherently vacant oxygen sites [21]. These oxygen vacancies can be hydrated through dissociative absorption of water and formation of protons, $OH_O^{\bullet}$.

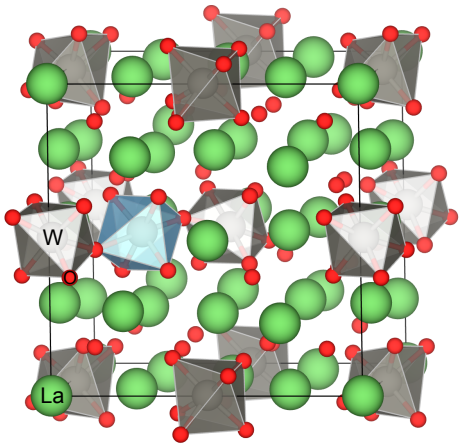

Figure 1: Structure of a unit cell of $La_{27}W_5O_{55.5-\delta}$ (La/W=5.4) showing excess W substituted on the La2 (24g) site (blue polyhedra). The figure is adapted from Ref. [18] and represents a specific configuration of cation and oxygen disorder.

Perovskite structured lanthanum chromite, $LaCrO_{3-\delta}$, is chemically stable over a wide range of p_{O_2} and exhibits significant p-type electronic conductivity from oxidizing to moderately reducing conditions when acceptor doped with, e.g., Ca or Sr on the La site [22,23]. The acceptor doped material exhibits appreciable O_2 permeability [24,25] and it has also been investigated as a hydrogen permeable membrane due to dissolution of protons in wet hydrogen containing atmospheres [8,26,27].

Hydrogen flux measurements of lanthanum tungstate and cercer membranes with $La_{0.87}Sr_{0.13}CrO_{3-\delta}$ (LSC) have revealed degradation of the flux over time, particularly evident at temperatures above 900 °C [13,28]. In the present study, we have investigated the stability of such cercer membranes under a chemical potential gradient by studying the H_2 permeability vs. time, and under a thermodynamic equilibrium by long-term annealing at high temperatures under various reducing conditions. In this respect, cercer materials of lanthanum tungstate (LW) or Mo-doped lanthanum tungstate (LWM) with various La/W ratios and LSC are employed. Based on characterization of structure, chemical composition and

microstructure, the degradation phenomena are discussed in terms of phase stability and defect chemistry of the materials.

2. Experimental

2.1 Sample preparation

Ceramic powders with nominal compositions $La_{26.96}W_{5.04}O_{55.6-\delta}$ (LW5.35), $La_{27.0}W_{3.50}Mo_{1.50}O_{55.5-\delta}$ (LWM5.40) and $La_{27.08}W_{3.44}Mo_{1.48}O_{55.5-\delta}$ (LWM5.50) were obtained from Marion Technologies (Verniolle, France) and $La_{0.87}Sr_{0.13}CrO_{3-\delta}$ (LSC) from Praxair (Indiana, USA). Mixtures of LW(M) with 40-50 wt% LSC were homogenized by ball milling overnight in a plastic container using zirconia balls. Symmetric cercer disc samples were prepared by uniaxial cold pressing at approx. 85 MPa (∅ = 13 and 21 mm) and the samples were sintered at 1475 °C in ambient air for 6 h with heating and cooling rates of 240 °C h^{-1}. The cercer samples are denoted according to their La/W ratio, e.g., LWM5.50-LSC for LWM5.50 with 40 wt% LSC, unless otherwise stated. The cercer disc samples for permeation measurements (∅ ≈ 16 mm after sintering) were gradually polished down to 3 µm surface roughness with SiC grinding paper and subsequently with a diamond abrasive. Slightly uniaxially pressed and similarly polished gold O-rings of 1 mm thickness were used to seal the samples to alumina support tubes (∅ = 13 mm).

2.2 Hydrogen permeation measurements

Hydrogen flux measurements were performed in a ProboStat measurement cell (NorECs, Norway). Mass flow controllers were utilized to supply $H_2/N_2/He$ feed gas mixtures and argon sweep gas at 50 and 25 ml min^{-1}, respectively. Wet feed and sweep gas mixtures were obtained by bubbling through a saturated KBr solution, yielding a water content of approx. 2.5%. The concentrations of H_2 permeate and He leakage were measured by a Varian CP-4900 gas chromatograph (GC). An alumina spring load assembly was used to provide a force of approx. 45 N on the sample against the gold gasket and alumina support tube. An S-type thermocouple was placed in the vicinity of the membrane and gold O-ring inside the measurement cell, which was inserted into a vertical tube furnace. A successful seal, as determined by a He leakage below the background He level in the GC, i.e., approx. 5 ppm, was typically obtained by heating the cell to 950 °C. Hydrogen fluxes were measured at 900 and 1000 °C with feed gas mixtures of 48.75% H_2, 2.5% H_2O, and 48.75% He, and a sweep of Ar with 2.5% H_2O for up to 1500 hours. For dense ceramic membranes, the H_2 permeability, J_{H_2}, is taken as the thickness normalized H_2 flux at given feed and sweep side conditions with units mL(STP) min^{-1} cm^{-1}. Since wet sweep gas was employed, the measured concentration of H_2 in the permeate stream can include contributions from water splitting and J_{H_2} therefore represents an apparent H_2 permeability.

2.3 Phase and microstructure characterization

Cercer samples were characterized as-sintered, after H_2 flux measurements and after annealing at 1000 °C in 49% H_2, 2.5% H_2O, rest Ar for 792 hours. The structure of the cercer components and possible degradation products was investigated by X-ray diffraction using a PANalytical Empyrean diffractometer with Cu Kα radiation and PIXcel^{3D} detector. The diffraction data were analyzed using the LeBail method as implemented in the Highscore software by PANalytical. Microstructure and chemical composition were studied by scanning electron microscopy (SEM) and energy dispersive spectroscopy (EDS) using a FEI Nova NanoSEM650 equipped with an OXFORD INSTRUMENTS X-Max50 EDS detector.

Scanning transmission electron microscopy (STEM) was used for imaging and elemental analysis by means of EDS of grain and phase boundaries in order to assess reactivity between the cercer constituents at these scales. Samples for STEM analysis were

prepared by grinding thin slices of sample mechanically to a thickness of around 150 µm. They were then dimpled to a central thickness of approx. 40 µm and thinned to electron transparency using a Gatan PIPS ion beam thinner operated at 3.5-2.5 kV and the samples were cooled during thinning. Analysis was performed using a JEOL 2100F transmission electron microscope equipped with an Oxford Instruments EDS system.

3. Results

Figure 2 shows the H_2 permeability as a function of time for LW5.35-LSC, LWM5.40-LSC and LWM5.50-LSC with wet 49% H_2 feed and wet Ar sweep. At 900 °C, there is a clear reduction in H_2 flux for the two latter membranes, while LW5.35-LSC exhibits a fairly stable permeability throughout the 250-hour measurements. Subsequently at 1000 °C, the flux degradation proceeds at a significantly faster rate, in particular during the first 200 hours for LWM5.40-LSC and LWM5.50-LSC. LW5.35-LSC exhibits a less significant degradation during the first 100 hours, and all membranes degrade at similar rate afterwards.

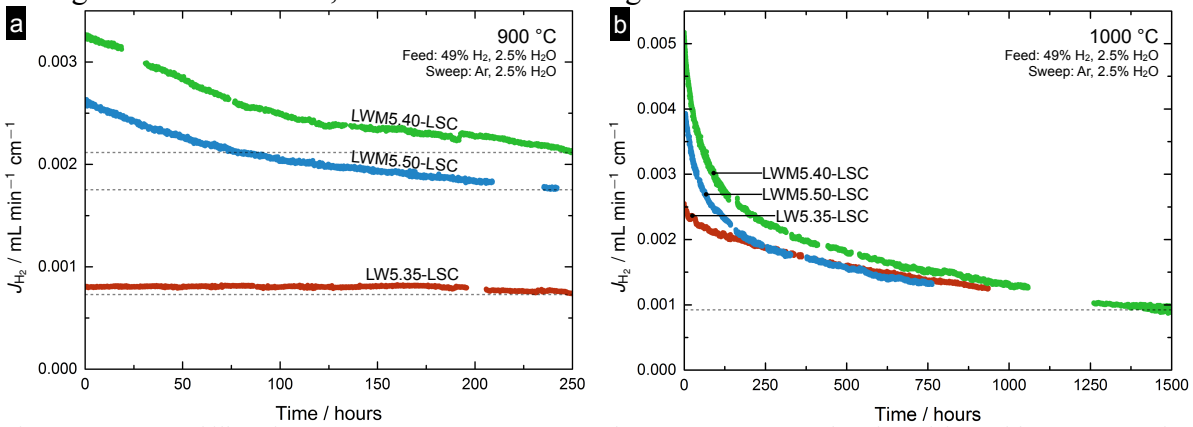

Figure 2: H_2 permeability of LW5.35-LSC, LWM5.40-LSC and LWM5.50-LSC as a function of time with wet 49% H_2 feed and wet Ar sweep at 900 °C (a) and subsequently at 1000 °C (b).

Figure 3 shows X-ray diffractograms of LW5.35-LSC, LWM5.40-LSC and LWM5.50-LSC samples as-sintered and after 792-hour annealing at 1000 °C in wet 49% H_2. All as-sintered samples exhibit trace amounts of La_2O_3, and the amount of La_2O_3 is significantly increased after 792 h annealing for all samples, although to a lesser extent for LW5.35-LSC. LW5.40-LSC exhibits an unidentified peak at approx. 29 ° (2 Theta) that disappears after annealing. The LSC phase was fitted to the $Pbnm$ space-group with lattice parameters a=5.46, b=7.74, c=5.51 Å for the as-sintered samples, and they remained essentially the same after the long-term annealing. The LW(M) phase was fitted to the $Fm\bar{3}m$ space-group with a lattice parameter of 11.17 Å for LW5.35-LSC and 11.18 Å for LWM5.40-LSC and LWM5.50-LSC due to the difference in La/W ratio and/or Mo content. The lattice parameters of the LWM phase exhibited a larger difference upon long-term annealing and were reduced to 11.15 Å for both LWM5.40-LSC and LWM5.50-LSC, while that of LW in LW5.35-LSC was only slightly reduced (still within 11.17 Å).

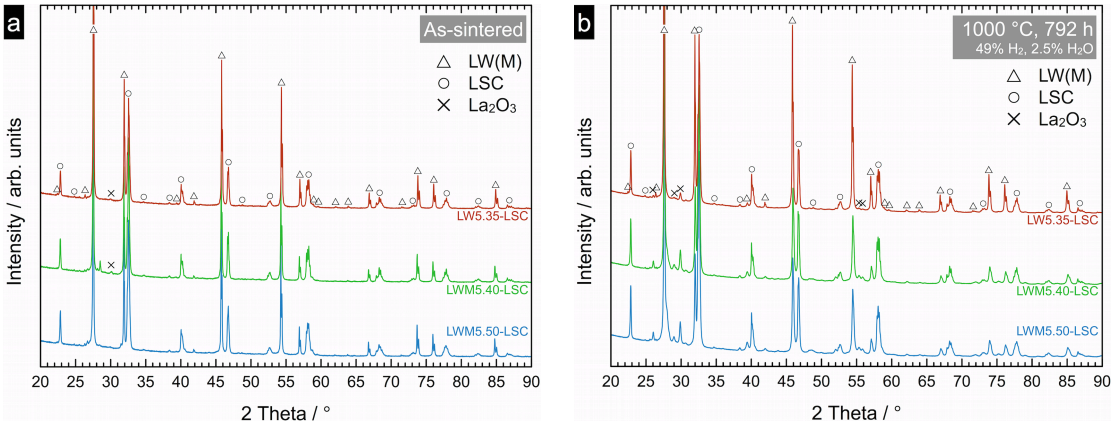

Figure 3: X-ray diffractograms of cercer samples as-sintered (a) and after a 792-hour annealing at 1000 °C in wet 49% H_2.

The microstructural characteristics of the surface and cross-section of the as-sintered and long-term annealed samples are exemplified for LWM5.40-LSC in Figure 4. While the LSC grains (dark) seem unchanged after annealing, the LWM grains undergo a restructuring particularly evident in the image of the polished surface after annealing (Figure 4, bottom). Considering the similar molar weight of LWM and La_2O_3, these phases would not be clearly distinguishable in these backscattered electron SEM images. The restructuring of the LWM phase may therefore be associated with La_2O_3 segregation as observed by XRD (c.f. Figure 3).

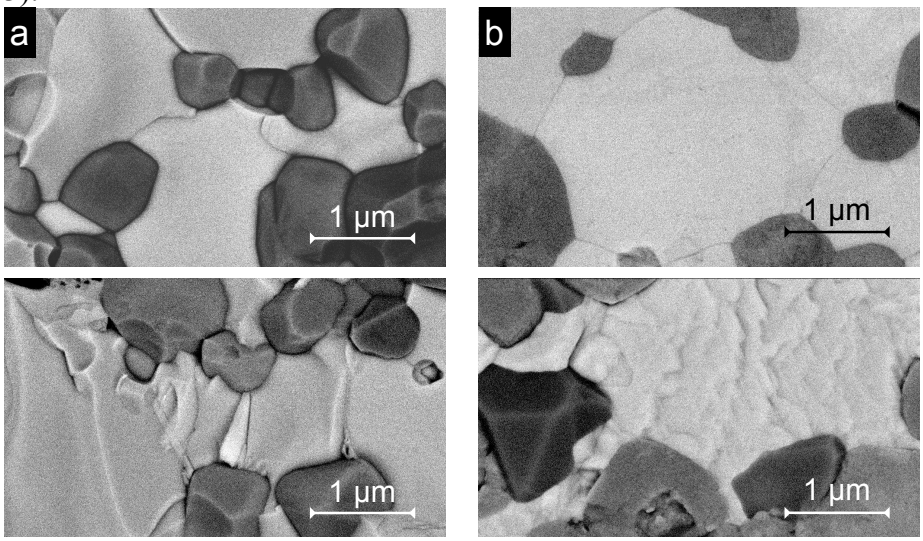

Figure 4: SEM micrographs of a fractured cross-section (a) and polished surface (b) of LWM5.40-LSC. The top images are of the as-sintered sample and the bottom images are taken after annealing at 1000 °C in wet 49% H_2 for 792 hours. The dark grains are LSC and the bright phase is LWM, and possibly La_2O_3 in the annealed and degraded samples.

In order to assess whether the H_2 flux degradation observed in Figure 2 was associated with changes in the bulk or only on the surface of the membrane, the degraded LWM5.40-LSC sample was re-polished and measured again. The hydrogen permeability of the re-polished sample at 1000 °C was estimated to be 1.03×10^{-3} mL min^{-1} cm^{-1} which is close to the last measured point at 1000 °C, 8.37×10^{-4}. Thus, the flux degradation seems to be a consequence of a process occurring throughout the bulk of the membrane material rather than kinetic demixing or decomposition which would be most evident at the surfaces.

3.1 Exposure to nominally dry H_2

Flux measurements were also performed on a LWM5.40-LSC membrane with 50 wt% LSC at 1000 °C for 96 hours. The H_2 permeability with wet 49% H_2 feed degraded from 0.0040 to 0.0020 mL min^{-1} cm^{-1} over the course of 15 hours when the membrane was exposed to a wet

feed of up to 88% H_2, i.e., similar to the initial degradation observed for LWM5.40-LSC and LWM5.50-LSC in Figure 2. The sample was partly exposed to nominally dry hydrogen during these flux measurements, which is critical for the understanding of the further characterization results.

The bright-field STEM image in Figure 5a shows that the as-sintered membrane is fully dense. By comparison, the dark-field image of Figure 5b shows pore formation at grain boundaries (particularly triple boundaries) after the flux measurements, with the pores appearing dark relative to the adjacent grains. The EDS map in Figure 5c indicates localised enrichment of W around the pores in Figure 5b which seems to be associated with the LWM phase.

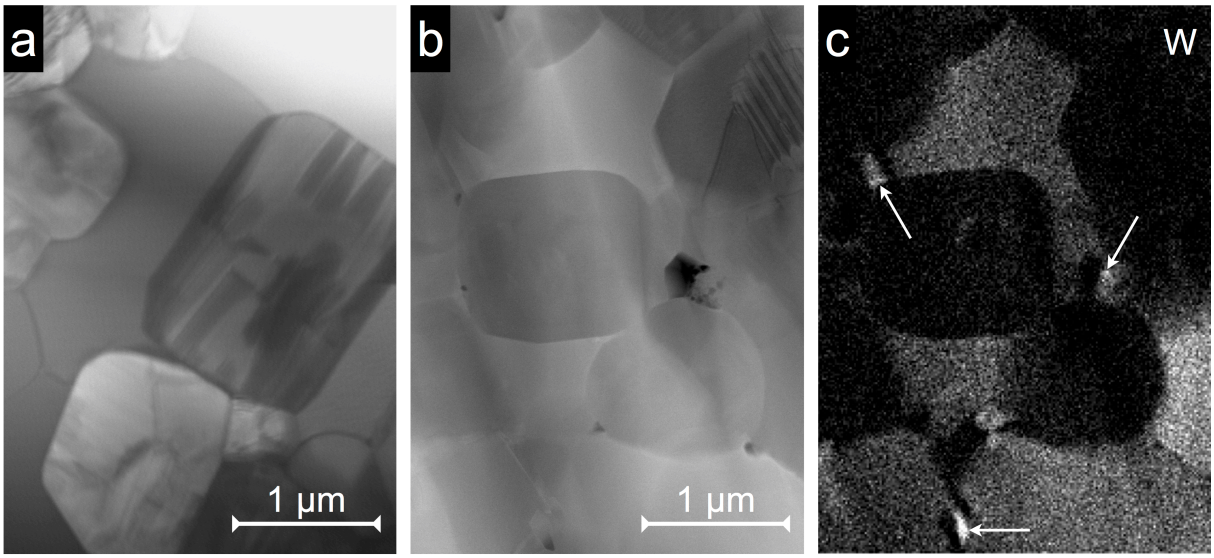

Figure 5: STEM bright-field image of LWM5.40-LSC (50 wt% LSC) as-sintered (a) and dark-field image after H_2 flux measurements at 1000 °C for 96 hours (b). Figure (c) shows an EDS map of W corresponding to the image in (b) with enriched areas highlighted by arrows.

Figure 6 shows a bright-field STEM image and corresponding EDS line scan across a LWM-LSC boundary in the degraded membrane; there is no clear indication of reaction or diffusion across the interface at this resolution which is limited by the fact that the sample is rather thick in the area that was analysed.

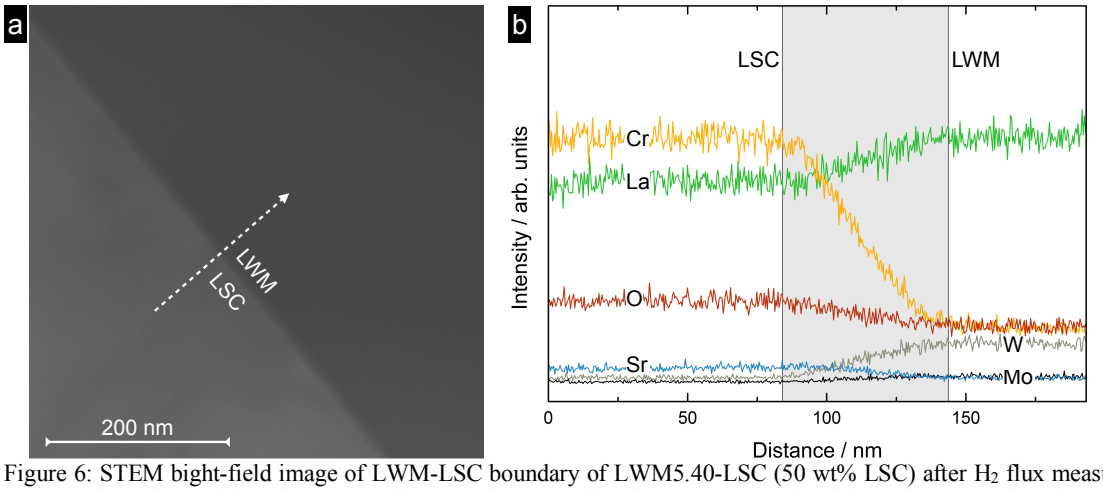

Figure 6: STEM bight-field image of LWM-LSC boundary of LWM5.40-LSC (50 wt% LSC) after H_2 flux measurements at 1000 °C for 96 hours (a) and corresponding EDS line scan (b). The apparent Cr signal from the LWM phase is caused by the La Lβ2 peak, which overlaps with the Cr Kα peak. This was confirmed by examination of individual spectra acquired from the two phases.

The LWM5.40-LSC (50 wt% LSC) sample was further annealed at 1000 °C in wet 49% H_2 for 258 hours and subsequently for an additional 1004 hours. The SEM surface images in Figure 7 reveal major changes in addition to the restructuring of the LWM grains (as seen in Figure 4): appearance of bright particles across the surface, and roughening of the initially smooth LSC grains. Judging by EDS analysis and the high intensity of the bright particles in the backscattered electron images, these particles were identified as metallic tungsten, which is the thermodynamically stable phase compared to WO_3 under the reducing conditions (p_{O_2}= 7×10^{-18} bar) [29]. There seems to be no significant further degradation after the additional 1004 h annealing. The same features were observed in SEM surface images of samples annealed in nominally dry hydrogen for only 24 hours.

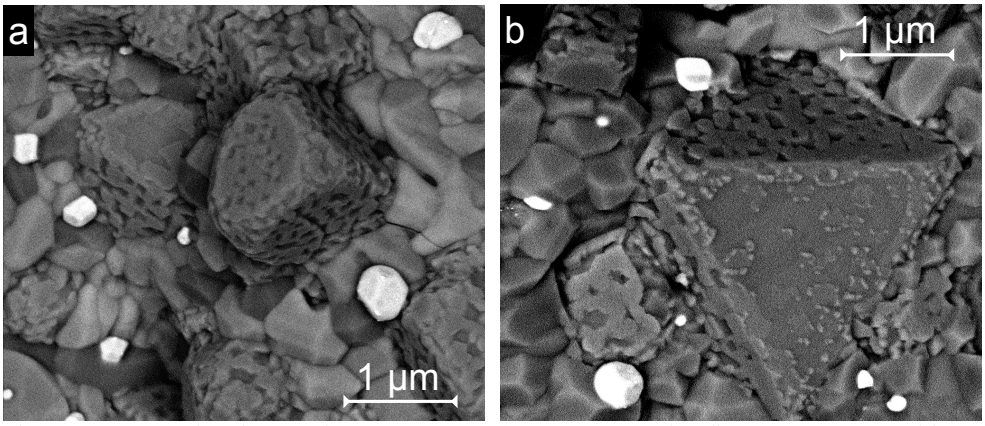

Figure 7: SEM surface image of LWM5.40-LSC (50 wt% LSC) after flux measurements with exposure to nominally dry hydrogen and annealing at 1000 °C in wet 49% H_2 for 258 hours (a) and additional 1004 hours (b), taken with the backscattered electron detector.

4. Discussion

The H_2 permeability of the cercer membranes can be understood from ambipolar conductivity where LW(M) mainly contributes with ionic conductivity of oxide ions and protons, while LSC mainly contributes with p-type electronic conductivity. The ionic conductivity of lanthanum tungstate increases with increasing La/W ratio due to the higher concentration of $v_O^{\bullet\bullet}$ and/or $OH_O^{\bullet}$ with lower $W_{La}^{\bullet\bullet\bullet}$ content [20].

As shown by XRD and SEM, the observed reduction in H_2 permeability is accompanied by segregation of La_2O_3. Considering the observed microstructural restructuring and change in the lattice parameter of the LW(M) phase, and that the amount of La_2O_3 segregation more or less follows the La/W ratio of the LW(M) phase, it is reasonable to assert that the segregated La_2O_3 originates from LW(M). The La/W ratio of the LW(M) phase is thereby decreased which can account for the degradation in H_2 permeability due to the lowered ionic conductivity. Notably, the H_2 permeability of all the membranes approaches a similar value after the initial stage of degradation, i.e., around 750 hours in Figure 2b. The degradation process can therefore be understood as a thermodynamic equilibration of the LW(M) phase under the flux measurement and annealing conditions. This is further supported by the fact that the degradation occurred throughout the bulk of the membrane as demonstrated by the unchanged H_2 permeability of the re-polished sample. For kinetic demixing or other surface sensitive degradation, one would expect the H_2 permeability of the re-polished sample to return to the initial value before degradation.

According to the La_2O_3–WO_3 phase diagram [20], the single-phase region for $La_{28-x}W_{4+x}O_{54+3x/2-\delta}V_{2-3x/2}$ in ambient air at 1000 °C corresponds to a La/W ratio lower than 5.3-5.4, while single-phase LW(M) can be obtained for higher La/W ratios at higher temperature. The conductivity of pure lanthanum tungstate samples has been reported to be stable at 1100 °C in wet H_2 for La/W ratios of 5.3 and 5.4 based on measurements carried out over 60 hours [20].

The present results show that phase instability and La_2O_3 segregation can occur for La/W ratios down to 5.35 at 1000 °C. Furthermore, the single-phase region may be shifted to slightly lower La/W ratio under reducing conditions as compared to oxidizing conditions of the phase diagram. The H_2 permeability of LWM5.40-LSC was lowered by a factor of 5.3 over the 1500-hour experiment in Figure 2b. This corresponds well with the approx. 4.8 times lower ionic conductivity of lanthanum tungstate with La/W ratio of 5.2 compared 5.4 [20], indicating that the final La/W ratio may be close to 5.2. Further evaluation of this material system for membrane applications should therefore assess material stability at lower temperatures so that the equilibrium La/W ratio and corresponding ionic conductivity and flux can be considered.

At this stage, it is not clear whether the slower degradation after about 300 hours in Figure 2b represents the same LW(M) phase equilibration or a different degradation process. The segregated La_2O_3 on surfaces and/or grain boundaries may contribute to lowering the H_2 permeability by blocking ionic and/or electronic transport. If so, redistribution of the segregated La_2O_3 may affect the H_2 permeability over time.

Evaporation of volatile constituents such as W or Mo [30] seems not to be significant for the investigated samples and conditions based on the unchanged microstructural features of the sample containing metallic W-particles after additional annealing (Figure 7). Segregation of similar W-rich particles, presumably metallic W, has been reported on the feed side of an LWM membrane after H_2 permeation measurements at 1000 °C with wet 90% H_2 in the feed [28], and for the similarly structured gadolinium tungstate, with a nominal Gd/W ratio of 6, treated in anhydrous NH_3 for 50 hours at 1000 °C [31].

5. Conclusions

The H_2 permeability of cercer membranes based on LW(M) with 40 wt.% LSC exhibits significant degradation under wet H_2 containing conditions at 900 and 1000 °C. The decrease of the flux was ascribed to the compositional instability of cation-disordered lanthanum tungstate at these operating temperatures while the material initially appears to be phase pure from sintering at higher temperature. The La/W ratio of the LW(M) phase is equilibrated by segregation of La_2O_3, leading to a lower ionic conductivity according to the materials inherent defect chemistry. The H_2 permeability of LWM5.40-LSC decreased by a factor of 5.3 over 1500 hours at 1000 °C, which corresponds well with the 5-time lower ionic conductivity of lanthanum tungstate with La/W ratio of 5.2 compared to 5.4. Partial decomposition and reduction of the lanthanum tungstate phase by exsolution of metallic tungsten particles was observed after exposure to nominally dry hydrogen.

6. Acknowledgements

This publication has been produced with support from the BIGCCS Centre, performed under the Norwegian research program *Centres for Environment-friendly Energy Research (FME)*. The authors acknowledge the following partners for their contributions: ConocoPhillips, Gassco, Shell, Statoil, TOTAL, ENGIE and the Research Council of Norway (193816/S60).

7. Referances

[1] R. Bredesen, K. Jordal, O. Bolland, High-temperature membranes in power generation with CO_2 capture, Chem. Eng. Process. Process Intensif. 43 (2004) 1129–1158.

[2] J.W. Phair, S.P.S. Badwal, Review of proton conductors for hydrogen separation, Ionics. 12 (2006) 103–115.

[3] F. Gallucci, E. Fernandez, P. Corengia, M. van Sint Annaland, Recent advances on membranes and membrane reactors for hydrogen production, Chem. Eng. Sci. 92 (2013) 40–66.

[4] G.Q. Lu, J.C. Diniz da Costa, M. Duke, S. Giessler, R. Socolow, R.H. Williams, et al., Inorganic membranes for hydrogen production and purification: a critical review and perspective., J. Colloid

Interface Sci. 314 (2007) 589–603.

[5] J.B. Smith, K.I. Aasen, K. Wilhelmsen, D. Käka, T. Risdal, A. Berglund, et al., Recent development in the HMR pre-combustion gas power cycle, Energy Procedia. 1 (2009) 343–351.

[6] L. Li, R.W. Borry, E. Iglesia, Design and optimization of catalysts and membrane reactors for the non-oxidative conversion of methane, Chem. Eng. Sci. 57 (2002) 4595–4604.

[7] T. Norby, R. Haugsrud, Dense Ceramic Membranes for Hydrogen Separation, in Membranes for Energy Conversion, Wiley-ECH Verlag Gmbh & Co KGaA, 2008.

[8] Y. Larring, C. Vigen, F. Ahouanto, M.-L. Fontaine, T. Peters, J.B. Smith, et al., Investigation of $La_{1-x}Sr_xCrO_{3-\delta}$ (x~0.1) as Membrane for Hydrogen Production, Membranes. 2 (2012) 665–686.

[9] Z. Li, C. Kjølseth, R. Haugsrud, Hydrogen permeation, water splitting and hydration kinetics in $Nd_{5.4}Mo_{0.3}W_{0.7}O_{12-\delta}$, J. Memb. Sci. 476 (2015) 105–111.

[10] A. Unemoto, A. Kaimai, K. Sato, K. Yashiro, H. Matsumoto, J. Mizusaki, et al., Hydrogen permeability and electrical properties in oxide composites, Solid State Ionics. 178 (2008) 1663–1667.

[11] W. Xing, G.E. Syvertsen, T. Grande, Z. Li, R. Haugsrud, Hydrogen permeation, transport properties and microstructure of Ca-doped $LaNbO_4$ and $LaNb_3O_9$ composites, J. Memb. Sci. 415-416 (2012) 878–885.

[12] S. Escolastico, S. Cecilia, C. Kjølseth, J.M. Serra, Outstanding hydrogen permeation through CO_2-stable dual phase ceramic membranes, Energy Environ. Sci. 7 (2014) 3736–3746.

[13] J.M. Polfus, W. Xing, M. Fontaine, C. Denonville, P.P. Henriksen, R. Bredesen, Hydrogen separation membranes based on dense ceramic composites in the $La_{27}W_5O_{55.5}$–$LaCrO_3$ system, J. Memb. Sci. 479 (2015) 39–45.

[14] S. Escolastico, J. Seeger, S. Roitsch, M. Ivanova, W. a Meulenberg, J.M. Serra, Enhanced H2 separation through mixed proton-electron conducting membranes based on $La_{5.5}W_{0.8}Mo_{0.2}O_{11.25-\delta}$., ChemSusChem. 6 (2013) 1523–32.

[15] J. Seeger, M.E. Ivanova, W. a Meulenberg, D. Sebold, D. Stöver, T. Scherb, et al., Synthesis and characterization of nonsubstituted and substituted proton-conducting La_6WO_{12-y}., Inorg. Chem. 52 (2013) 10375–86.

[16] V. Gil, J. Gurauskis, C. Kjølseth, K. Wiik, M.-A. Einarsrud, Hydrogen permeation in asymmetric $La_{28-x}W_{4+x}O_{54+3x/2}$ membranes, Int. J. Hydrogen Energy. 38 (2013) 3087–3091.

[17] A. Magrasó, C. Frontera, D. Marrero-López, P. Núñez, New crystal structure and characterization of lanthanum tungstate "La_6WO_{12}" prepared by freeze-drying synthesis., Dalt. Trans. (2009) 10273–83.

[18] A. Magrasó, J.M. Polfus, C. Frontera, J. Canales-Vázquez, L.-E. Kalland, C.H. Hervoches, et al., Complete structural model for lanthanum tungstate: a chemically stable high temperature proton conductor by means of intrinsic defects, J. Mater. Chem. 22 (2012) 1762.

[19] L. Kalland, A. Magraso, A. Mancini, C. Tealdi, L. Malavasi, Local Structure of Proton-Conducting Lanthanum Tungstate $La_{28-x}W_{4+x}O_{54+\delta}$: a Combined Density Functional Theory and Pair Distribution Function Study, Chem. Mater. (2013).

[20] A. Magrasó, R. Haugsrud, Effects of the La/W ratio and doping on the structure, defect structure, stability and functional properties of proton-conducting lanthanum tungstate $La_{28-x}W_{4+x}O_{54+\delta}$. A review., J. Mater. Chem. A. (2014) 12630–12641.

[21] S. Erdal, L.-E. Kalland, R. Hancke, J. Polfus, R. Haugsrud, T. Norby, et al., Defect structure and its nomenclature for mixed conducting lanthanum tungstates $La_{28-x}W_{4+x}O_{54+3x/2}$, Int. J. Hydrogen Energy. 37 (2012) 8051–8055.

[22] N. Sakai, T. Kawada, H. Yokokawa, Sinterability and electrical conductivity of calcium-doped lanthanum chromites, J. Mater. Sci. 25 (1990) 4531–4534.

[23] P. Devi, M. Subba Rao, Preparation, Structure, and Properties of Strontium-Doped Lanthanum Chromites: $La_{1-x}Sr_xCrO_3$, J. Solid State Chem. 98 (1992) 237–244.

[24] B.A. van Hassel, T. Kawada, N. Sakai, H. Yokokawa, M. Dokiya, Oxygen permeation modelling of $La_{1-y}Ca_yCrO_{3-\delta}$, Solid State Ionics. 66 (1993) 41–47.

[25] T. Kawada, T. Horita, N. Sakai, H. Yokokawa, M. Dokiya, Experimental determination of oxygen permeation flux through bulk and grain boundary of $La_{0.7}Ca_{0.3}CrO_3$, Solid State Ionics. 79 (1995) 201–207.

[26] S. Julsrud, B.E. Vigeland, Solid multicomponent mixed proton and electron conducting membrane, EP

Patent 1448293, 2007.

[27] C.K. Vigen, R. Haugsrud, Hydrogen flux in $La_{0.87}Sr_{0.13}CrO_{3-\delta}$, J. Memb. Sci. 468 (2014) 317–323.

[28] E. Vøllestad, C.K. Vigen, A. Magrasó, R. Haugsrud, Hydrogen permeation characteristics of $La_{27}Mo_{1.5}W_{3.5}O_{55.5}$, J. Memb. Sci. 461 (2014) 81–88.

[29] C.W. Bale, P. Chartrand, S.A. Degterov, G. Eriksson, K. Hack, R. Ben Mahfoud, et al., FactSage thermochemical software and databases, Calphad Comput. Coupling Phase Diagrams Thermochem. 26 (2002) 189–228.

[30] G. a. Greene, C.C. Finfrock, Vaporazation of tungsten in flowing steam at high temperatures, Exp. Therm. Fluid Sci. 25 (2001) 87–99.

[31] J.M. Polfus, Nitrogen Defects in Oxides, M.Sc thesis, University of Oslo (2009) http://urn.nb.no/URN:NBN:no-22600.